Am J Transl Res 2019;11(9):5375-5389
www.ajtr.org /ISSN:1943-8141/AJTR0100199

Original Article

Early administration of cold water and adipose derived mesenchymal stem cell derived exosome effectively protects the heart from ischemia-reperfusion injury

Han-Tan Chai[1*], Jiunn-Jye Sheu[2,4,5], John Y Chiang[3,9], Pei-Lin Shao[7], Shun-Cheng Wu[8], Yi-Ling Chen[1,4], Yi-Chen Li[1], Pei-Hsun Sung[1,5], Fan-Yen Lee[2,4,5,10], Hon-Kan Yip[1,4,5,6,7*]

[1]Division of Cardiology, Department of Internal Medicine, [2]Division of Thoracic and Cardiovascular Surgery, Department of Surgery, Kaohsiung Chang Gung Memorial Hospital and Chang Gung University College of Medicine, Kaohsiung 83301, Taiwan; [3]Department of Computer Science and Engineering, National Sun Yat-Sen University, Kaohsiung, Taiwan; [4]Institute for Translational Research in Biomedicine, [5]Center for Shockwave Medicine and Tissue Engineering, Kaohsiung Chang Gung Memorial Hospital, Kaohsiung 83301, Taiwan; [6]Department of Medical Research, China Medical University Hospital, China Medical University, Taichung 40402, Taiwan; [7]Department of Nursing, Asia University, Taichung 41354, Taiwan; [8]Orthopaedic Research Center, College of Medicine, [9]Department of Healthcare Administration and Medical Informatics, Kaohsiung Medical University, Kaohsiung, Taiwan; [10]Tri-Service General Hospital, National Defense Medical Center, Taipei 11490, Taiwan. [*]Equal contributors.

Received June 6, 2019; Accepted July 29, 2019; Epub September 15, 2019; Published September 30, 2019

Abstract: This study tested the hypothesis that early administration with cold water (CW)-assisted adipose-derived mesenchymal stem cell (ADMSC)-derived exosome (Exo) therapy was superior to either one on protecting the heart against ischemia-reperfusion (IR) (i.e., by ligation of 50 minutes and relieved by day 5 prior to euthanizing the animals) injury. Adult-male SD rats (n=30) were equally categorized into groups 1 (sham-operated control), 2 (IR), 3 (IR + CW), 4 (IR + Exo) and 5 (IR + CW-Exo). The left ventricular ejection fraction (LVEF) was highest in group 1, lowest in group 2, and significantly higher in group 5 than in groups 3 and 4, but no difference between groups 3 and 4 (all P<0.001). The protein expressions of oxidative-stress (NOX-1/NOX-2/NOX-4/oxidized protein), apoptotic/mitochondrial-damaged (mitochondrial-Bax/caspase 3/PARP/p53/cytosolic-cytochrome-C) and inflammatory (IL-1β/TNF-α/NF-κB/MMP-9) biomarkers, and cellular-stress response signaling (PI3K/Akt/GSK3β and p-m-TOR) showed an opposite pattern, whereas the anti-oxidants (SIRT1/SIRT3), anti-inflammation (IL-10) and IKB-α/p-AMKP/mitochondrial-cytochrome-C exhibited an identical pattern to the LVEF among the five groups (all P<0.0001). The cellular expressions of inflammation (CD68), total cellular ROS (i.e., stained by H_2DCFDA) and the LV infarct/fibrotic/collagen-deposition areas displayed an opposite pattern, whereas the cell gap junction (coonexin 43) and sarcomere length exhibited an identical pattern of LVEF among the five groups (all P<0.0001). Conclusion: Combined CW-exosome therapy markedly protected the heart against IR injury.

Keywords: Ischemia-reperfusion, hypothermic therapy, exosome, cell-stress signaling, inflammation, oxidative stress

Introduction

Swift restoration of the blood flow by opening the occluded artery (i.e. called reperfusion therapy) is the key to protect the deterioration of the ischemia-related organ dysfunction [1-3]. However, reperfusion therapy will always introduce an inevitable reperfusion injury [4-7]. Primary percutaneous coronary intervention (PCI) is a pathological condition of myocardial ischemia-reperfusion (IR) injury characterized by loss of the coronary blood supply to the myocardium followed by restoration of coronary artery perfusion in setting of acute myocardial infarction (AMI) during primary coronary intervention [8]. Thus, reperfusion has been described as the “double edged sword” [4].

In fact, myocardial IR injury contributes to unfavorable cardiac events in settings of myocardial ischemia/AMI, cardiovascular surgical interventions, cardiogenic shock, or any cause of circu-

latory arrest [9-13]. Abundant data have shown that IR injury involves not only intracellular injury processes, generation of reactive oxygen species (ROS)/oxygen free radicals, but also harmfully inflammatory and immune reactions [8, 11, 14-19]. Furthermore, ROS are essential contributors to the opening of the mitochondrial permeability transition pore, resulting in the rapidly release of cytochrome C (i.e., an indicator of mitochondrial damage) and cell death [20, 21], ultimately causing loss of heart contractile function [22, 23]. Despite decades of intensive research, advanced pharmaco-therapeutic strategies and state-of-the-art coronary interventions, effective treatments for myocardial IR injury are regrettably lacking [17, 20, 21, 24]. Accordingly, there is an urgent need for a safe and efficacious treatment modality.

Therapeutic hypothermia is used for patients following both out-of-hospital and in-hospital cardiac arrest for purposes of preserving organ viability [25]. Growing data have shown that among patients with in-hospital cardiac arrest, use of therapeutic hypothermia compared with usual care was associated with a higher likelihood of survival to hospital discharge and favorable neurological survival [26-29]. The underlying mechanisms of mild hypothermia (usually at 4°C) for protecting the neuropeptide effect have been proposed as holding the ability to up-regulate the expression of anti-apoptotic gene Bcl-2, and decrease the levels of some inflammatory chemokines (such as IL-8, MCP-1 and COX-2) in endothelial cells [30], inducing the expression of cold-inducible RNA-binding protein to inhibit cell apoptosis induced by tumor necrosis factor-α via the activation of extracellular signal-regulated kinase [31] as well as reducing ROS/free radical production and mitochondrial damage through inhibiting mitochondrial permeability transition pore, apoptosis and inflammation [30, 31]. Additionally, recent study has further identified that possible molecular mechanism for cellular protective effect of mild hypothermia involved the PI3K-Akt-GSK3β signal pathway and anti-apoptotic pathway [32].

Interestingly, previous studies have demonstrated that mesenchymal stem cell-derived exosomes have distinctive properties, namely, promotion of angiogenesis, immunomodulation and paracrine effects that preserve organ function following injury in preclinical studies [33-36]. Additionally, our recent studies have shown that adipose-derived mesenchymal stem cell (ADMSC) derived exosome (Exo) ($ADMSC^{Exo}$) has capacity of anti-inflammation and immunomodulatory effect [37, 38]. Furthermore, our studies have further revealed that $ADMSC^{Exo}$ treatment effectively attenuated brain, kidney, liver and lung IR injury [38-41]. Based on the aforementioned findings, we tested the hypothesis that combined hypothermia and exosome would be superior to either one alone for protecting the heart against IR-induced injury.

Materials and methods

Ethics

All animal experiment procedures were approved by the Institute of Animal Care and Use Committee at Kaohsiung Chang Gung Memorial Hospital (Affidavit of Approval of Animal Use Protocol No. 2017092103) and performed in accordance with the Guide for the Care and Use of Laboratory Animals.

Animals were housed in an Association for Assessment and Accreditation of Laboratory Animal Care International (AAALAC; Frederick, MD, USA)-approved animal facility in our hospital with free access to water and standard animal chow in a room with controlled temperature at 24°C and 12-hour light-dark cycles.

Induction of acute myocardial ischemia-reperfusion injury and animal grouping

Pathogen-free, adult male Sprague-Dawley (SD) rats (n=30) weighing 320-350 g (Charles River Technology, BioLASCO, Taiwan) were utilized in the present study. The procedure and protocol for myocardial IR injury were based on our recent report [42]. In detail, all animals were placed under anesthesia with 2.0% inhalational isoflurane on a warming pad at 37°C for the IR procedure. Under sterile conditions, the heart was exposed via a left thoracotomy. IR injury was induced by ligating the left coronary artery (LCA) for 40 minutes with a 7-0 prolene suture, 3 mm distal to the margin of the left atrium. Regional myocardial ischemia was verified by observing a rapid color change from pink to dull red over the anterior surface of the left ventricle and swift development of akinesia and dilatation over the affected region. Rats receiving thoracotomy only without ischemia induction served as sham-operated controls (SC). The knot was then released after 40-min-

ute ischemia, followed by 5 days reperfusion. The rats were sacrificed at day 5 after IR procedure, and hearts were harvested.

The animals were divided into five groups: group 1 (SC), group 2 (IR only), group 3 [IR + cold water (CW) at 4°C was injected into LCA (12 μl), followed by infusion of the same volume of CW (i.e., 14 μl) for each of the ischemic area for a total of three areas (i.e., total volume was 54 μl for one animal) at 40 minutes just at the beginning of reperfusion], group 4 [IR + $AMDSC^{Exo}$ (total 52 ug) was intra-coronary injection (10 μg) and implanted into three ischemic areas (i.e., 14 μg/each site) just at the beginning of reperfusion] and group 5 (IR + combination $CW\text{-}AMDSC^{Exo}$). The dosage of exosome was based on our previous reports [38-41] with minimal modification.

Functional assessment with echocardiography

The procedure and protocol for echocardiography have been described in our previous report [42]. Transthoracic echocardiography was performed in each group prior to and on day 5 after myocardial IR induction. The procedure was performed by an animal cardiologist blinded to the experimental design using an ultrasound machine (Vevo 2100, Visualsonics). M-mode standard two-dimensional (2D) left parasternal-long axis echocardiographic examination was conducted. Left ventricular internal dimensions [end-systolic diameter (ESD) and end-diastolic diameter (EDD)] were measured at papillary level of left ventricle, according to the American Society of Echocardiography leading-edge method using at least three consecutive cardiac cycles. LVEF was calculated as follows: $LVEF\ (\%) = [(LVEDD^3 - LVEDS^3)/LVEDD^3] \times 100\%$.

Western blot analysis of heart tissues

Western blot analysis was performed as described previously [39, 41, 42]. In detail, equal amounts (50 μg) of protein extracts were loaded and separated by SDS-PAGE. Separated proteins were transferred to PVDF membranes, and nonspecific sites were blocked by incubation in blocking buffer [5% nonfat dry milk in T-TBS (TBS containing 0.05% Tween 20)] overnight. The membranes were incubated with the indicated primary antibodies [mitochondrial Bax (1:1000, Abcam), cleaved poly (ADP-ribose) polymerase (PARP) (1:1000, Cell Signaling), caspase 3 (1:1000, Cell Signaling), tumor necrotic factor (TNF)-α (1:1000, Cell Signaling), matrix metalloproteinase (MMP)-9 (1:3000, Abcam), interleukin (IL)-1β (1:1000, Cell Signaling), nuclear factor (NF)-κB (1:1000, Abcam), IL-10 (1:1000, Abcam), NADPH oxidase (NOX)-1 (1:1500, Sigma), NOX-2 (1:500, Sigma), NOX-4 (1:1000, Abcam), cytosolic cytochrome C (1:1000, BD), mitochondrial cytochrome C (1:1000, BD), p53 (1:1000, Cell Signaling), phosphorylated (p) nuclear factor-κB (p-NF-κB) (1:1000, Cell Signaling), nuclear factor of kappa light polypeptide gene enhancer in B-cells inhibitor, alpha (IKB-α) (1:1000, Cell Signaling), Phosphoinositide 3-kinase (PI3K) (1:5000, Abcam), Akt (1:1000, Cell Signaling), glycogen synthase kinase 3β (GSK3β) (1:2000, Abcam), AMP-activated protein kinase (AMKP) (1:1000, Cell Signaling), phosphorylated mammalian target of rapamycin (p-m-TOR) (1:1000, Cell Signaling), SIRT1 (1:4000, Abcam) and SIRT3 (1:500, Abcam) for 1 hour at room temperature. Horseradish peroxidase-conjugated anti-rabbit IgG (1:2000, Cell Signaling) was used as a secondary antibody. Immuno-reactive bands were visualized by enhanced chemiluminescence (ECL; Amersham Biosciences) and digitized using Labwork software (UVP).

Assessment of total intracellular ROS test by H_2DCFDA

For determining the fluorescent intensity of ROS in myocardium, six additional animals were used in each study group. The protocol and procedure of this examination have been described in our previous report [42] with some modifications. In detail, by day 5 after DCM induction, 2',7'-dichlorodihydrofluorescin diacetate (H_2DCFDA, Molecular Probes) was dissolved in DMSO at a concentration of 25 mg/mL. After being diluted with 50% ethanol to a final concentration of 2.5 mg/mL, it was administered intravenously at a dose of 6 μg/g body weight to each animal. The rats were sacrificed 30 minutes following H_2DCFDA administration.

The hearts were harvested, excised and sectioned. Totally three 3-mm-thick sections were obtained from each heart. All sections were examined under fluorescent microscope with a magnification of 400 × (Olympus). Image analysis was performed offline using Image J (National Institutes of Health, USA). This formula was employed to calculate integrated fluorescent density, i.e., integrated fluorescent density = area of selected cell × mean gray value.

Oxidative stress reaction in LV myocardium

Expression of oxidative stress proteins has been described previously [39, 41, 42]. Oxyblot Oxidized Protein Detection Kit was purchased from Chemicon (S7150). DNPH derivatization was carried out using 6 μg of protein for 15 minutes according to the manufacturer's instructions. One-dimensional electrophoresis was carried out on 12% SDS/polyacrylamide gel after DNPH derivatization. Proteins were transferred to nitrocellulose membranes, which were then incubated in the primary antibody solution (anti-DNP 1:150) for 2 hours, followed by incubation in secondary antibody solution (1:300) for 1 hour at room temperature. Immuno-reactive bands were visualized by ECL (Amersham Biosciences) and digitized using Labwork software (UVP).

Immunohistochemical (IHC) and immunofluorescent (IF) staining

Re-hydrated paraffin sections were treated with 3% H_2O_2 for 30 minutes and incubated with Immuno-Block reagent (BioSB, Santa Barbara, CA, USA) for 30 minutes at room temperature. Sections were then incubated with primary antibodies against CD68 (1:100, ab31630, Abcam), connexin 43 (1:200, MAB3067, Merck millipore), sarcomere (1:500, IMG-80152, IMGENEX), Masson's trichrome (ScyTek, Trichrome stain kit) and Sirius red (Direct Red 80, Sigma-Aldrich). Three sections of heart specimens from each rat were analyzed. For quantification, three randomly selected HPFs (100 ×, 200 × or 400 × for IHC and IF studies) were analyzed in each section. The mean number of positively-stained cells per HPF for each animal was determined by summation of all numbers divided by 9.

Histological quantification of myocardial fibrosis/Infarct and collagen deposition

The relevant procedure and protocol were detailed in our previous reports [42, 43]. Briefly, hematoxylin and eosin (H&E) and Masson's trichrome staining were used to identify the infarct area and fibrosis of LV myocardium, respectively. Three serial sections of LV myocardium in each animal were prepared at 4 μm thickness by Cryostat (Leica CM3050S). The integrated areas (μm^2) of infarction and fibrosis on each section were calculated using the Image Tool 3 (IT3) image analysis software (University of Texas, Health Science Center, San Antonio, UTHSCSA; Image Tool for Windows, Version 3.0, USA). Three randomly selected high-power fields (HPFs) (100 ×) were analyzed in each section. After determining the number of pixels in each infarct and fibrotic area per HPF, the numbers of pixels obtained from three HPFs were calculated. The procedure was repeated in two other sections for each animal. The mean pixel number per HPF for each animal was then determined by calculating all pixel numbers and dividing by 9. The mean integrated area (μm^2) of fibrosis in LV myocardium per HPF was obtained using a conversion factor of 19.24 (since 1 μm^2 corresponded to 19.24 pixels). This method was also applied for identification of connexin 43 (Cx43) expression in myocardium.

To analyze the extent of collagen synthesis and deposition, cardiac paraffin sections (6 μm) were stained with picrosirius red (1% Sirius red in saturated picric acid solution) for one hour at room temperature. The sections were then washed twice with 0.5% acetic acid. After dehydration in 100% ethanol, the sections were cleaned with xylene and mounted in a resinous medium. High power fields (× 100) of each section were used to identify Sirius red-positive areas in each section. Analysis of the collagen deposition area in LV myocardium was performed analogously.

Statistical analysis

Quantitative data are expressed as means ± SD. Statistical analysis was performed by ANOVA followed by Bonferroni multiple-comparison post hoc test. SAS statistical software for Windows version 8.2 (SAS institute, Cary, NC, USA) was utilized. A probability value <0.05 was considered statistically significant.

Results

*LVEF and infarction area by day 5 after IR procedure (**Figure 1**)*

By day 0 prior to the acute IR procedure, the LVEF was similar among the five groups. However, by day 5 after IR procedure, the LVEF was highest in group 1 (i.e., SC), lowest in group 2 (IR) and significantly higher in group 5 (IR + CW-ADMSC^{Exo}) than in group 3 (IR + CW) and group 4 (IR + ADMSC^{Exo}), but no difference between the latter two groups. On the other

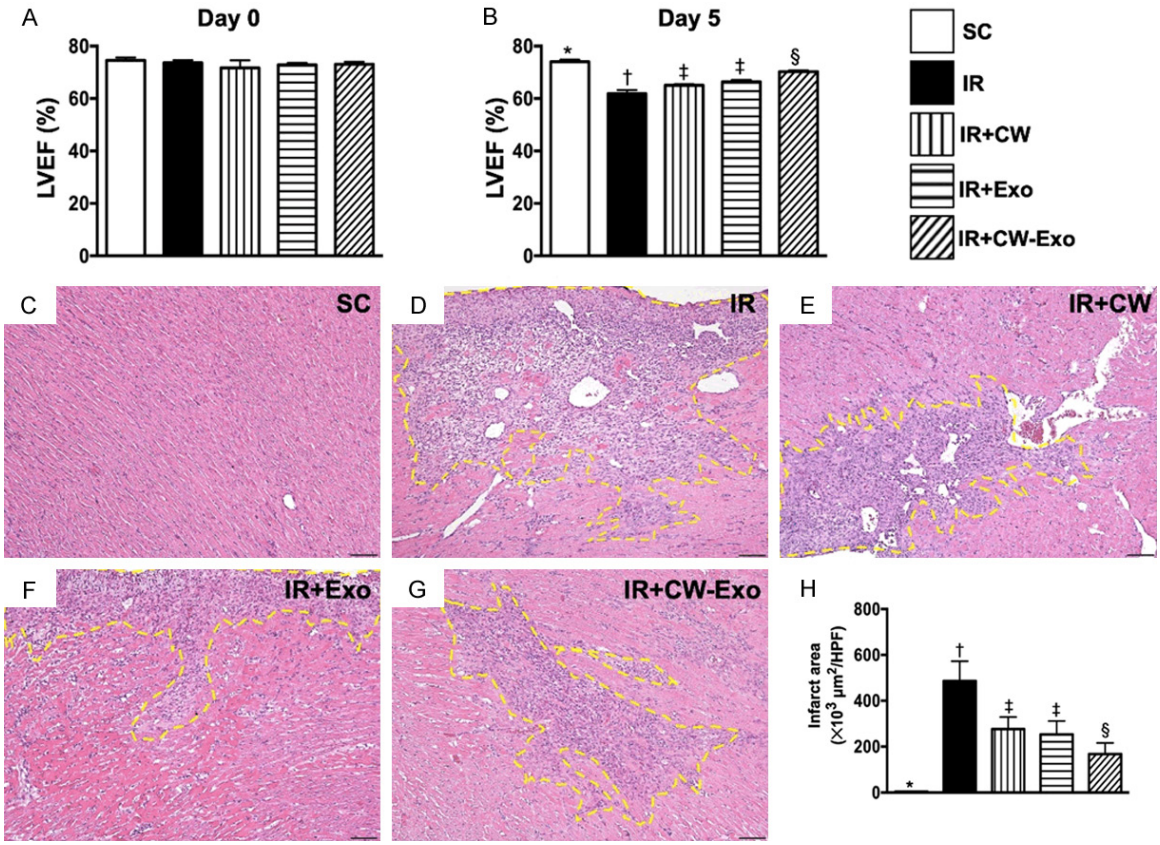

Figure 1. Time intervals of LVEF and infarction area by day 5 after IR procedure. A. By day 0 prior to IR procedure, the analytical results of left ventricular ejection fraction (LVEF), P>0.5. B. By day 5 after IR procedure, analytical result of LVEF, * vs. other groups with different symbols (†, ‡, §), P<0.001. C-G. Illustrating the microscopic finding (100 ×) of H.E. stain for identification of infarct area (yellow-dotted line). H. Analytical result of infarct area, * vs. other groups with different symbols (†, ‡, §), P<0.0001. All statistical analyses were performed by one-way ANOVA, followed by Bonferroni multiple comparison post hoc test (n=6 for each group). Symbols (*, †, ‡, §) indicate significance (at 0.05 level). HPF = high-power field; SC = sham-operated control; IR = ischemia reperfusion; CW = cold water; Exo = adipose-derived mesenchymal stem cell-derived exosome.

hand, the H.E stain showed that LV infarction area exhibited an opposite pattern of LVEF among the five groups. Accordingly, these functional (i.e., 2-D echo finding) and pathological (i.e., microscopic finding) parameters proved that early administration of CW-ADMSC^{Exo} therapy notably protected the heart from acute IR injury.

*Histopathological findings of LV myocardium by day 5 after IR procedure (**Figure 2**)*

The Masson's trichrome stain demonstrated that the fibrotic area in LV myocardial ischemic zone was highest in group 2, lowest in group 1, and significantly lower in group 5 than in groups 3 and 4, but it did not differ between these latter two groups. Additionally, Sirius-red stain showed that the collagen-deposition area in LV myocardial ischemic region exhibited an identical pattern of fibrosis among the five groups.

*Inflammatory cell infiltration and ROS in LV myocardium by day 5 after IR procedure (**Figure 3**)*

The IF microscopic findings demonstrated that cellular expressions of CD68, an indicator of inflammation, were highest in group 2, lowest in group 1, and significantly lower in group 5 than in groups 3 and 4, but both showed no difference between groups 3 and 4. Additionally, the IF microscopy demonstrated that the intensity of ROS expression (i.e., after H_2DCFDA staining) in LV myocardium, an indicator of total cellular expression of ROS, exhibited a similar pattern to that of CD68+ cells among the five

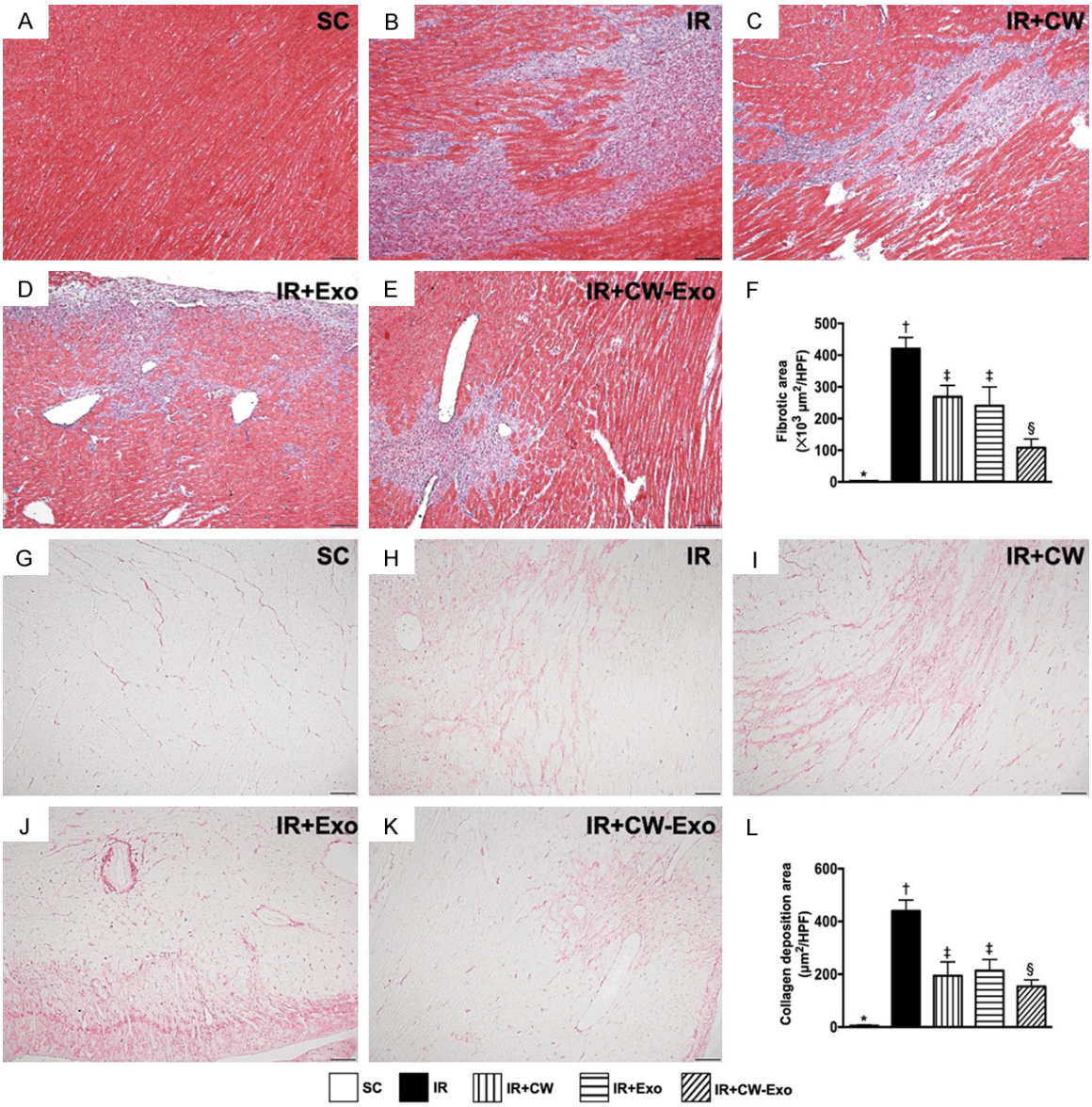

Figure 2. Histopathological findings of LV myocardium by day 5 after IR procedure. A-E. Illustrating the microscopic finding (100 ×) of Masson's trichrome stain for identification of fibrotic area (blue color). F. Analytical result of fibrotic area, * vs. other groups with different symbols (†, ‡, §), P<0.0001. G-K. Illustrating the microscopic finding (100 ×) of Sirius-red stain for identification of collagen-deposition area (pink color). L. Analytical result of collagen-deposition area, * vs. other groups with different symbols (†, ‡, §), P<0.0001. Scale bars in lower right corner represent 50 μm. All statistical analyses were performed by one-way ANOVA, followed by Bonferroni multiple comparison post hoc test (n=6 for each group). Symbols (*, †, ‡, §) indicate significance (at 0.05 level). SC = sham-operated control; IR = ischemia reperfusion; CW = cold water; Exo = adipose-derived mesenchymal stem cell-derived exosome.

groups, except for that the ORS was notably lower in group 4 than in group 3.

*Cellular expressions of connexin 43 and sarcomere length in LV myocardium by day 5 after IR procedure (**Figure 4**)*

The IF microscopic finding revealed that the expression of connexin 43 in LV myocardium, an indicator of cellular gap junction for cell to cell communication, was highest in group 1, lowest in group 2, and significantly higher in group 5 than in groups 3 and 4, but it showed no difference between groups 3 and 4. Additionally, The sarcomere length of LV myocardium displayed an identical pattern to connexin 43, suggesting an early stage of intrinsic response of increasing LV myocardial hypertrophy/contractility following AMI for compensated

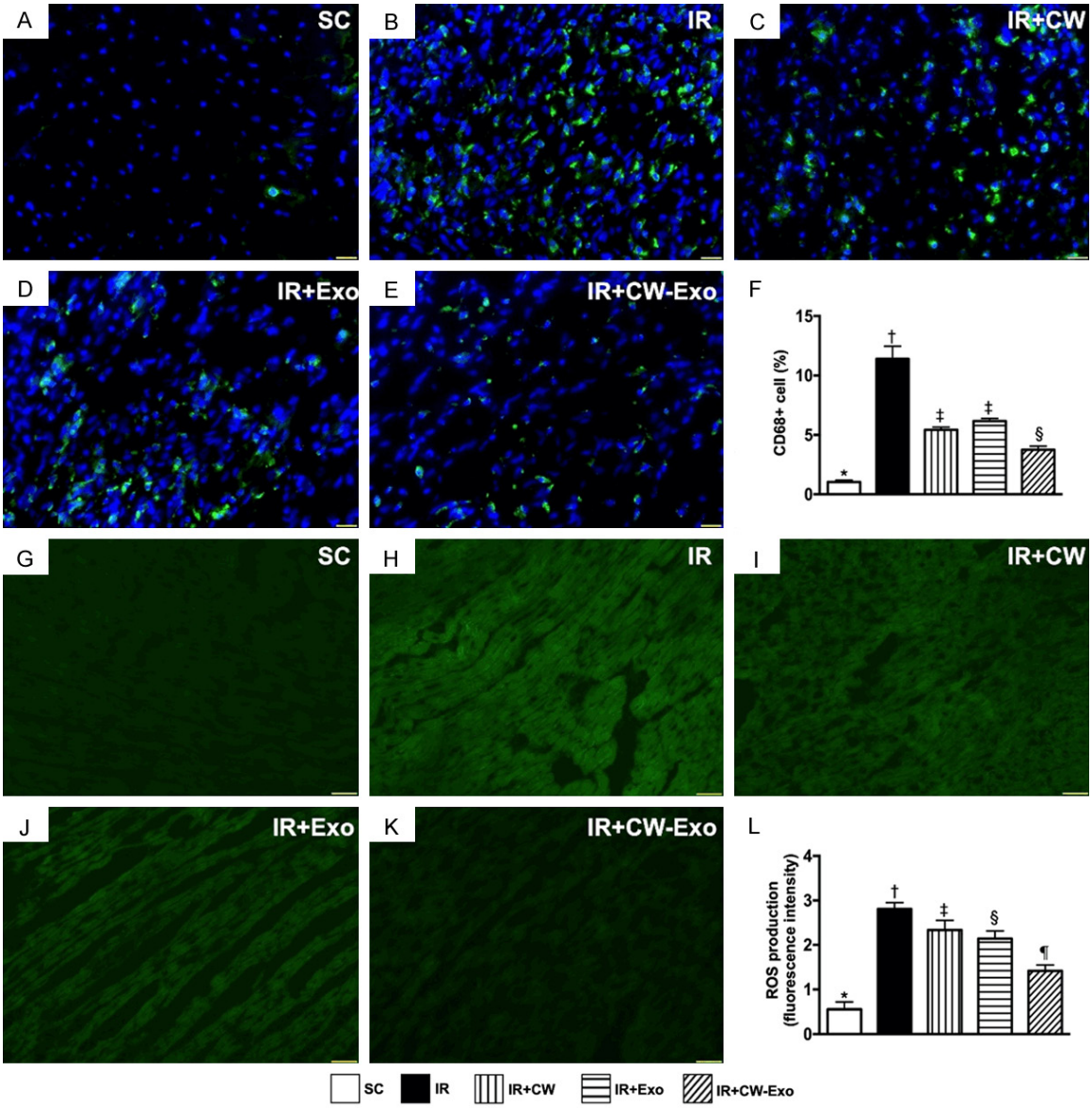

Figure 3. Inflammatory cell infiltration and ROS in LV myocardium by day 5 after IR procedure. A-E. Illustrating the immunofluorescent (IF) microscopic finding (400 ×) for identification of CD68+ cells (green color). F. Analytical result of number of positively stained CD68 cells, * vs. other groups with different symbols (†, ‡, §), P<0.0001. Scale bars in lower right corner represent 20 μm. G-K. Illustrating the IF microscopic finding (400 ×) for identification of fluorescent intensity of H_2DCFDA stain [i.e., an indicator of tissue reactive oxygen species (ROS)] (green color). L. Analytical result of fluorescent intensity ROS in kidney tissue, * vs. other groups with different symbols (†, ‡, §, ¶), P<0.0001. All statistical analyses were performed by one-way ANOVA, followed by Bonferroni multiple comparison post hoc test (n=6 for each group). Symbols (*, †, ‡, §, ¶) indicate significance (at 0.05 level). SC = sham-operated control; IR = ischemia reperfusion; CW = cold water; Exo = adipose-derived mesenchymal stem cell-derived exosome.

LV dysfunction/heart failure that was attenuated by CW-exosome treatment.

*The protein expressions of oxidative stress, antioxidant and inflammation in LV myocardium by day 5 after IR procedure (**Figures 5** and **6**)*

The protein expressions of NOX-1, NOX-2, NOX-4 and oxidized protein, four indicators of oxidative stress, were highest in group 2, lowest in group 1 and significantly lower in group 5 than in groups 3 and 4, but no difference between groups 3 and 4 (**Figure 5**). However, the protein expressions of SIRT1 and SIRT3, two indices of anti-oxidants, displayed an opposite pattern of oxidative stress among the five groups (**Figure 5**). On the other hand, the protein expressions

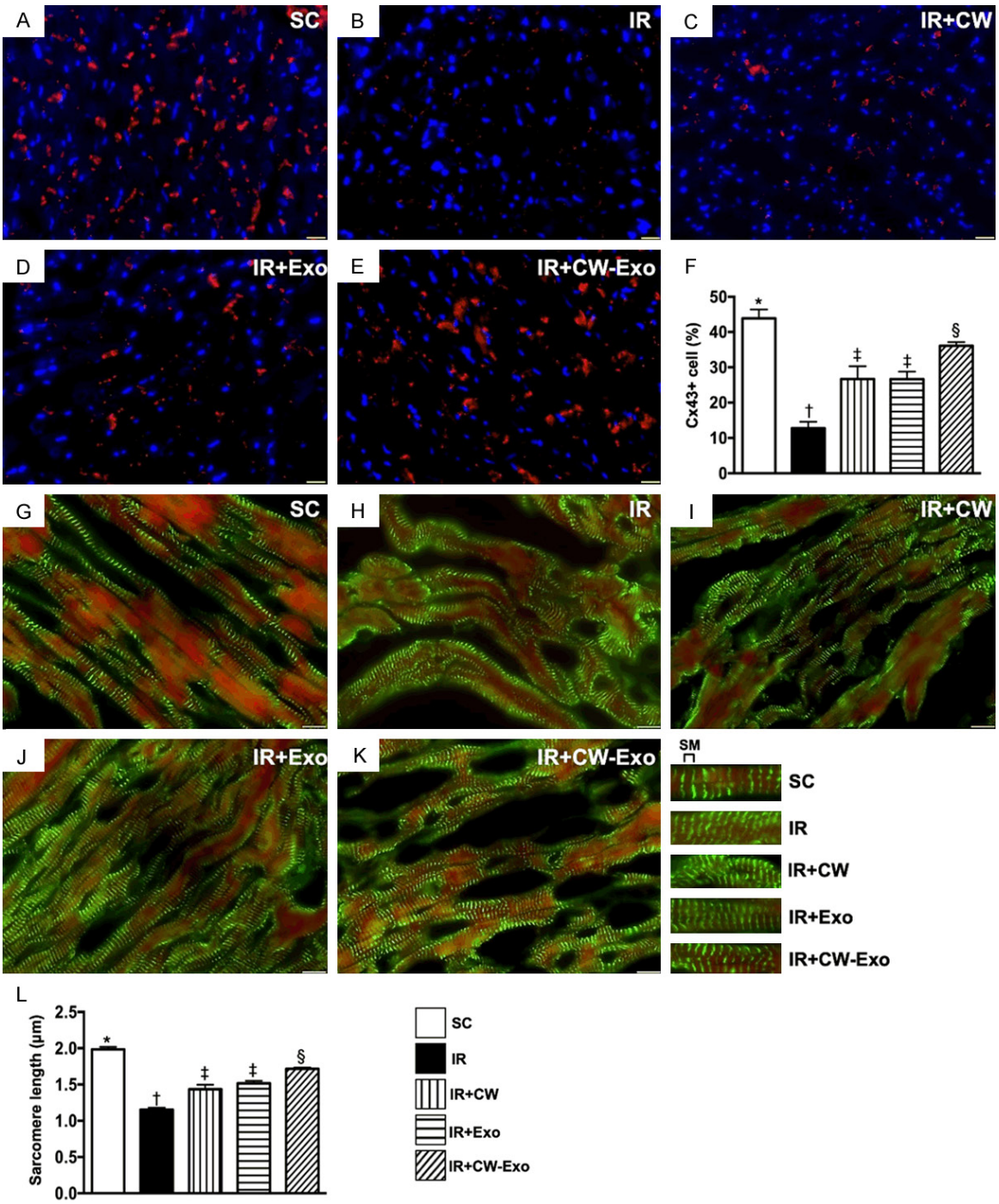

Figure 4. Cellular expressions of connexin 43 and sarcomere length in LV myocardium by day 5 after IR procedure. A-E. Illustrating the immunofluorescent (IF) microscopic finding (400 ×) for identification of the expression of connexin 43 (Cx43) in LV myocardium (red color). F. Analytical result of accumulated Cx43 area (%), * vs. other groups with different symbols (†, ‡, §), P<0.0001. Scale bars in lower right corner represent 20 μm. G-K. illustrating the IF microscopic finding (400 ×) for identification of sarcomere (SM) length (1000 ×). L. Analytical result of SM length, * vs. other groups with different symbols (‡, ‡), P<0.0001. All statistical analyses were performed by one-way ANOVA, followed by Bonferroni multiple comparison post hoc test (n=6 for each group). Symbols (*, †, ‡, §) indicate significance (at 0.05 level). SM = sarcomere length; SC = sham-operated control; IR = ischemia reperfusion; CW = cold water; Exo = adipose-derived mesenchymal stem cell-derived exosome.

of IL-1β, TNF-α, p-NF-κB, and MMP-9, four inflammatory biomarkers, revealed an identical pattern, whereas the protein expression of IKB-α, its function is to inhibit the NF-κB transcrip-

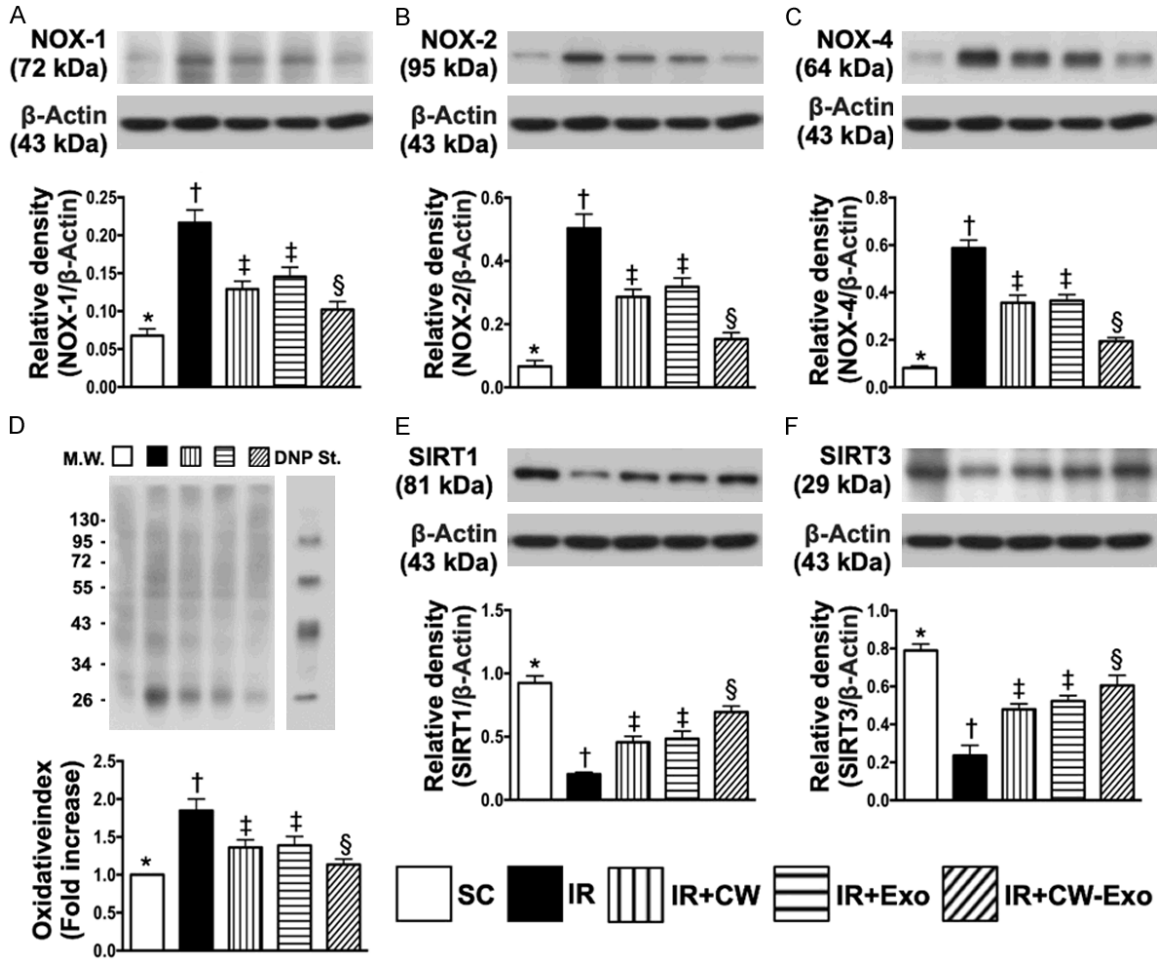

Figure 5. The protein expressions of oxidative stress and antioxidants in LV myocardium by day 5 after IR procedure. A. Protein expression of NOX-1, * vs. other groups with different symbols (†, ‡, §), P<0.0001. B. Protein expression of NOX-2, * vs. other groups with different symbols (†, ‡, §), P<0.0001. C. Protein expression of NOX-4, * vs. other groups with different symbols (†, ‡, §), P<0.0001. D. The oxidized protein expression, * vs. other groups with different symbols (†, ‡, §), P<0.0001 (Note: the right and left lanes shown on the upper panel represent protein molecular weight marker and control oxidized molecular protein standard, respectively). M.W = molecular weight; DNP = 1-3 dinitrophenylhydrazone. E. Protein expression of SIRT1, * vs. other groups with different symbols (†, ‡, §), P<0.0001. F. Protein expression of SIRT3, * vs. other groups with different symbols (†, ‡, §), P<0.0001. All statistical analyses were performed by one-way ANOVA, followed by Bonferroni multiple comparison post hoc test (n=6 for each group). Symbols (*, †, ‡, §) indicate significance (at 0.05 level). SC = sham-operated control; IR = ischemia reperfusion; CW = cold water; Exo = adipose-derived mesenchymal stem cell-derived exosome.

tion factor, and protein expression of IL-10, an indicator of anti-inflammation, exhibited an opposite pattern of oxidative stress among the five groups (**Figure 6**).

*The protein expressions of apoptotic and mitochondrial damaged biomarkers in LV myocardium by day 5 after IR procedure (**Figure 7**)*

The protein expressions of mitochondrial-Bax and cleaved caspase 3, two indicators of apoptotic biomarkers, were highest in group 2, lowest in group 1 and significantly lower in group 5 than in groups 3 and 4, but there was no difference between groups 3 and 4. Additionally, the protein expressions of cleaved PARP and p53, another two indicators of cellular apoptotic/death biomarkers, were highest in group 2, lowest in group 1, significantly lower in group 5 than in groups 3 and 4, and significantly lower in group 4 than in group 3. Furthermore, the protein expression of cytosolic cytochrome C, a mitochondrial damaged marker, displayed an identical pattern, whereas the protein expres-

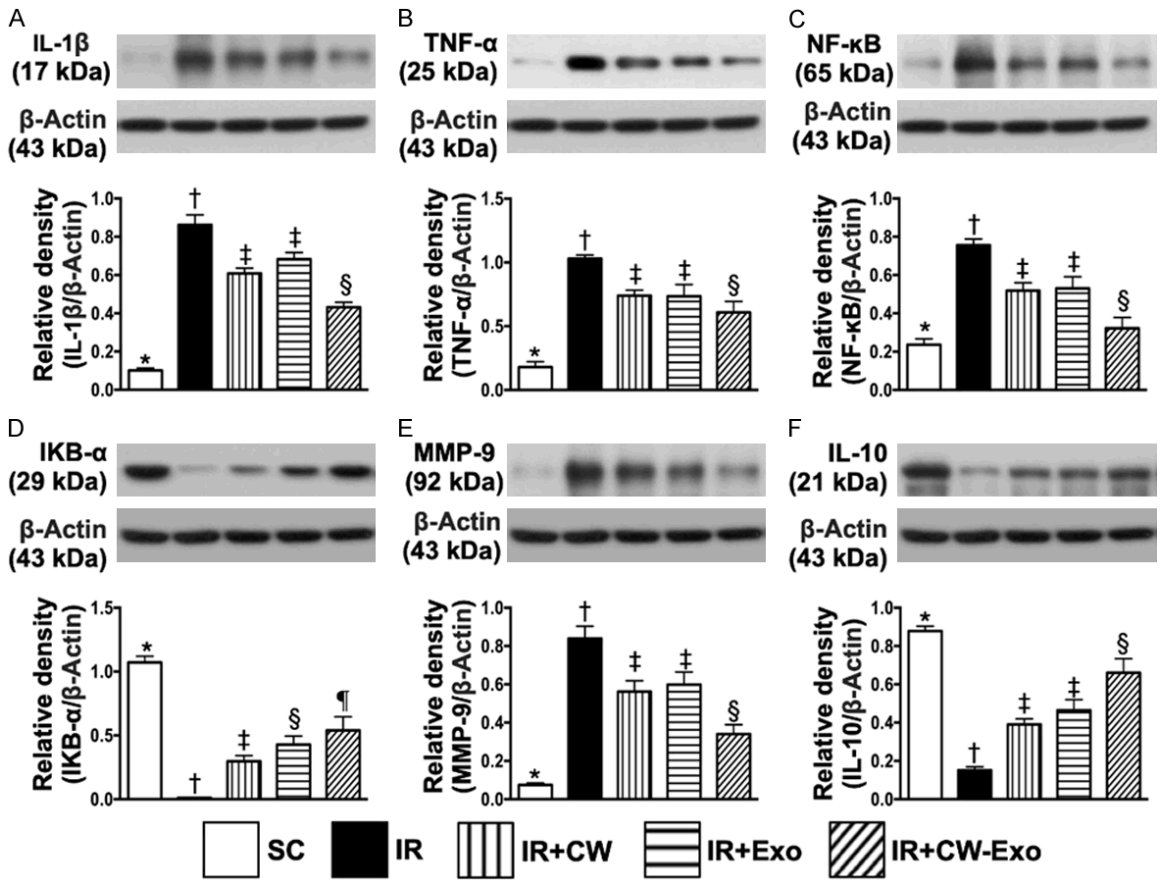

Figure 6. Protein expressions of inflammatory and anti-inflammatory mediators in LV myocardium by day 5 after IR procedure. A. Protein expression of interleukin (IL)-1β, * vs. other groups with different symbols (†, ‡, §), P<0.0001. B. Protein expression of tumor necrosis factor (TNF)-α, * vs. other groups with different symbols (†, ‡, §), P<0.0001. C. Protein expression of phosphorylated (p) nuclear factor-κB (p-NF-κB), * vs. other groups with different symbols (†, ‡, §, ¶), P<0.0001. D. Nuclear factor of kappa light polypeptide gene enhancer in B-cells inhibitor, alpha (IKB-α), * vs. other groups with different symbols (†, ‡, §), P<0.0001. E. Protein expression of matrix metalloproteinase (MMP)-9, * vs. other groups with different symbols (†, ‡, §), P<0.0001. F. Protein expression of IL-10, * vs. other groups with different symbols (†, ‡, §), P<0.0001. All statistical analyses were performed by one-way ANOVA, followed by Bonferroni multiple comparison post hoc test (n=6 for each group). Symbols (*, †, ‡, §, ¶) indicate significance (at 0.05 level). SC = sham-operated control; IR = ischemia reperfusion; CW = cold water; Exo = adipose-derived mesenchymal stem cell-derived exosome.

sion of mitochondrial cytochrome C, an indicator of mitochondrial integrity, exhibited an opposite pattern of p53 among the five groups.

*The protein expressions of cell-stress response signaling in LV myocardium by day 5 after IR procedure (**Figure 8**)*

The protein expressions of PI3K, p-Akt, GSK3β, p-m-TOR and p-AMKP, five cell-stress response signaling biomarkers, were highest in group 2, lowest in group 1, and significantly lower in group 5 than in groups 3 and 4, but no difference between groups 3 and 4, suggesting an intrinsic cellular response to ischemic stimulation in IR setting that was ameliorated by CW-Exo treatment.

Discussion

This study which investigated the therapeutic impact of CW-Exo on protecting the heart from IR injury yielded several striking implications. First, CW was comparable to Exo therapy for preserving the LVEF in setting of acute IR injury in rat. Second, combined CW-Exo added an additional benefit to preserving the LVEF and cardiac architectural integrity after acute IR procedure. Third, the results of the present study demonstrated that CW-Exo therapy on

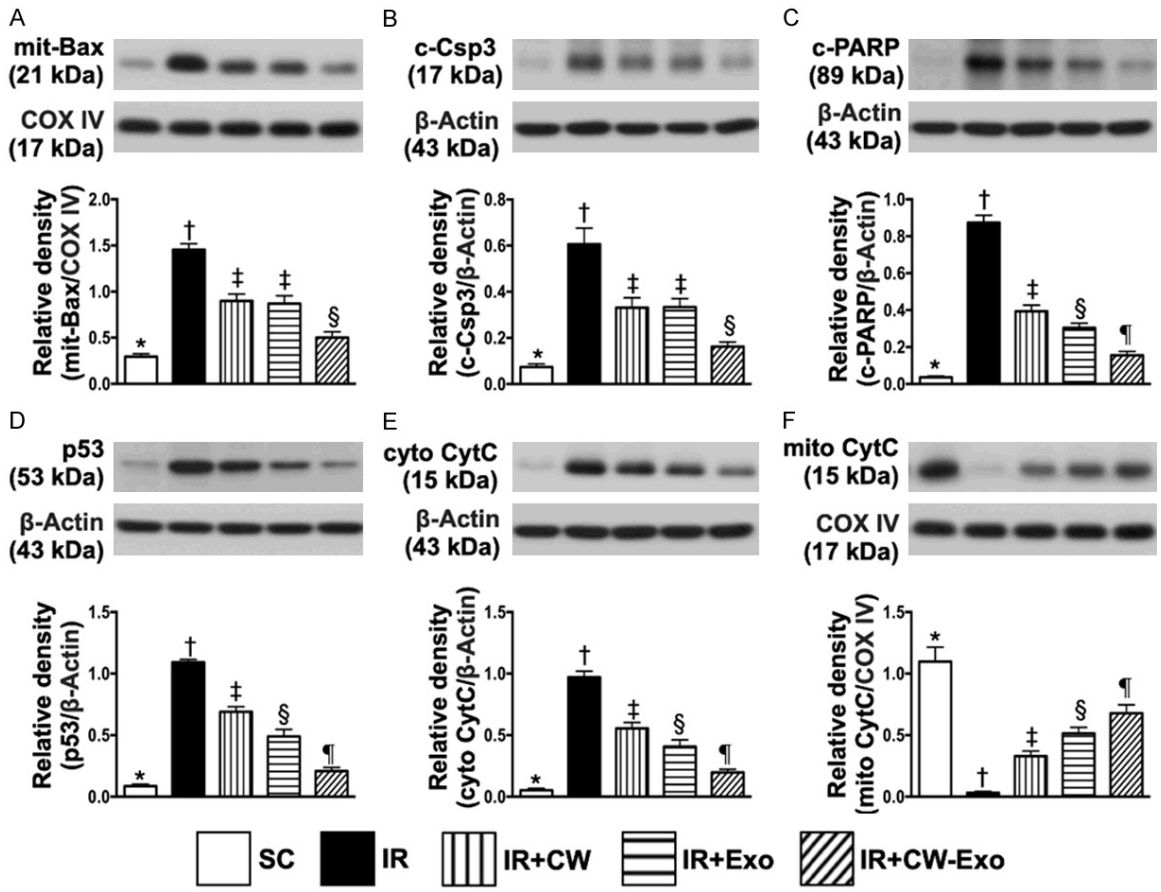

Figure 7. Protein expressions of apoptotic and mitochondrial damaged biomarkers in LV myocardium by day 5 after IR procedure. A. Protein expression of mitochondrial-Bax (mito-Bax), * vs. other groups with different symbols (†, ‡, §), P<0.0001. B. Protein expression of cleaved caspase 3 (c-Csp3), * vs. other groups with different symbols (†, ‡, §), P<0.0001. C. Protein expression of cleaved poly (ADP-ribose) polymerase (c-PARP), * vs. other groups with different symbols (†, ‡, §, ¶), P<0.0001. D. Protein expression of p53, * vs. other groups with different symbols (†, ‡, §, ¶), P<0.0001. E. Protein expression of cytosolic cytochrome C (cyt-CytoC), * vs. other groups with different symbols (†, ‡, §, ¶), P<0.0001. F. Protein expression of mitochondrial cytochrome C (mito-CytoC), * vs. other groups with different symbols (†, ‡, §, ¶), P<0.0001. All statistical analyses were performed by one-way ANOVA, followed by Bonferroni multiple comparison post hoc test (n=6 for each group). Symbols (*, †, ‡, §, ¶) indicate significance (at 0.05 level). SC = sham-operated control; IR = ischemia reperfusion; CW = cold water; Exo = adipose-derived mesenchymal stem cell-derived exosome.

protecting the heart function against IR injury was mainly through inhibiting oxidative stress/inflammatory signaling that regulated the intrinsic cell-stress response pathway.

Interestingly, clinical studies have previously shown that hypothermic therapy offered a higher likelihood of survival to hospital discharge and favorable neurological survival [26-29] mainly through the preservation of vital organ viability [25] in critical patients. Additionally, a couple of experimental studies have clearly shown that MSC-derived Exo therapy effectively protected the ischemic-related/IR injured organ dysfunction [38-41]. The most important finding in the present study was that as compared with IR only animals, the LVEF (i.e., functional interpretation) was significantly improved, whereas the infarct, collagen-deposition and fibrotic areas (i.e., histopathological features) were substantially reduced in those of CW or Exo treated IR animals and these parameters were further altered in those of IR animals after receiving combined CW-Exo therapy. Accordingly, our findings, in addition to extending the results of previous studies [25-29, 38-41], highlight that this therapeutic modality (i.e., CW-Exo) may be potential for those of severe myocardial IR patients who are refractory to conventional therapy.

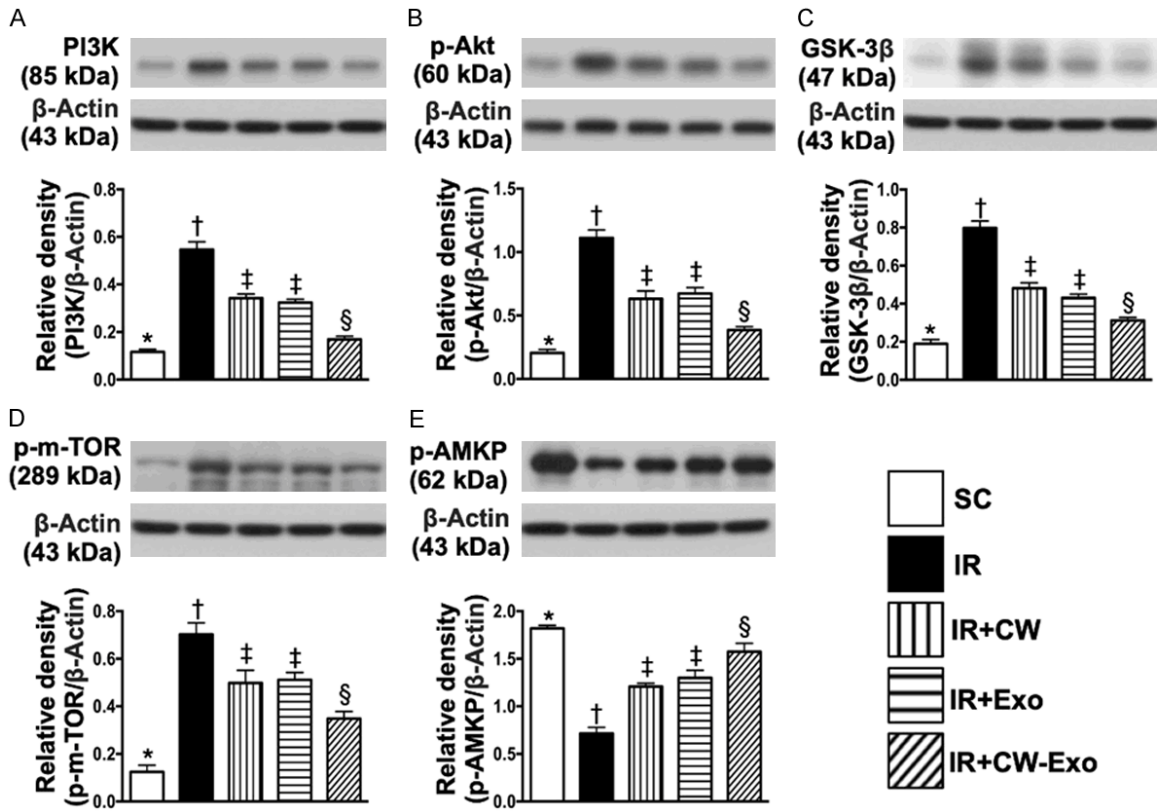

Figure 8. Protein expressions of cell-stress response signaling in LV myocardium by day 5 after IR procedure. A. Protein expression of Phosphoinositide 3-kinase (PI3K), * vs. other groups with different symbols (†, ‡, §), P<0.0001. B. Protein expression of phosphorylated (p)-Akt, * vs. other groups with different symbols (†, ‡, §), P<0.0001. C. Protein expression of glycogen synthase kinase 3β (GSK3β), * vs. other groups with different symbols (†, ‡, §), P<0.0001. D. Protein expression of p-m-TOR, * vs. other groups with different symbols (†, ‡, §), P<0.0001. E. Protein expression of p-AMP-activated protein kinase (AMKP), * vs. other groups with different symbols (†, ‡, §), P<0.0001. All statistical analyses were performed by one-way ANOVA, followed by Bonferroni multiple comparison post hoc test (n=6 for each group). Symbols (*, †, ‡, §) indicate significance (at 0.05 level). SC = sham-operated control; IR = ischemia reperfusion; CW = cold water; Exo = adipose-derived mesenchymal stem cell-derived exosome.

Associations among oxidative stress, inflammatory reaction, and mitochondrial and organ damages have been keenly investigated [16, 19, 20, 38-43]. One essential finding in the present study was that as compared with SC, the oxidative stress, inflammation, apoptosis and mitochondrial damage were substantially increased in IR animals. These findings, in addition to being consistent with the results of previous studies [38-43], could powerfully explain why the LVEF was notably reduced and infarcted/fibrotic/collagen-deposition areas were substantially increased in those of IR animals. However, these cellular-molecular perturbations and infarcted/fibrotic/collagen-deposition areas were remarkably suppressed and LVEF was markedly increased in those of IR animals after receiving CW or Exo therapy and further altered in these animals after receiving CW-Exo therapy. Our findings, therefore, strengthened the conclusions from previous studies [16, 19, 20, 38-43].

The underling mechanisms of hypothermia therapy for protecting the vital organs [25] and giving the favorable neurological survival [26-29] have been revealed to be very complicated, including anti-apoptosis, suppression of inflammatory chemokines [30], induction of expression of cold-inducible RNA-binding protein, activation of extracellular signal-regulated kinase [31] and inhibition of ROS/free radical production, mitochondrial damage [30, 31] as well as possible regulation of PI3K-Akt-GSK3β signal pathway [32]. On the other hand, our previous studies have identified that Exo therapy protected the ischemia/IR-related organ dysfunction was mainly through inhibitions of inflammation and oxidative stress and upregulation of immunomodulation [38-41]. A principal find-

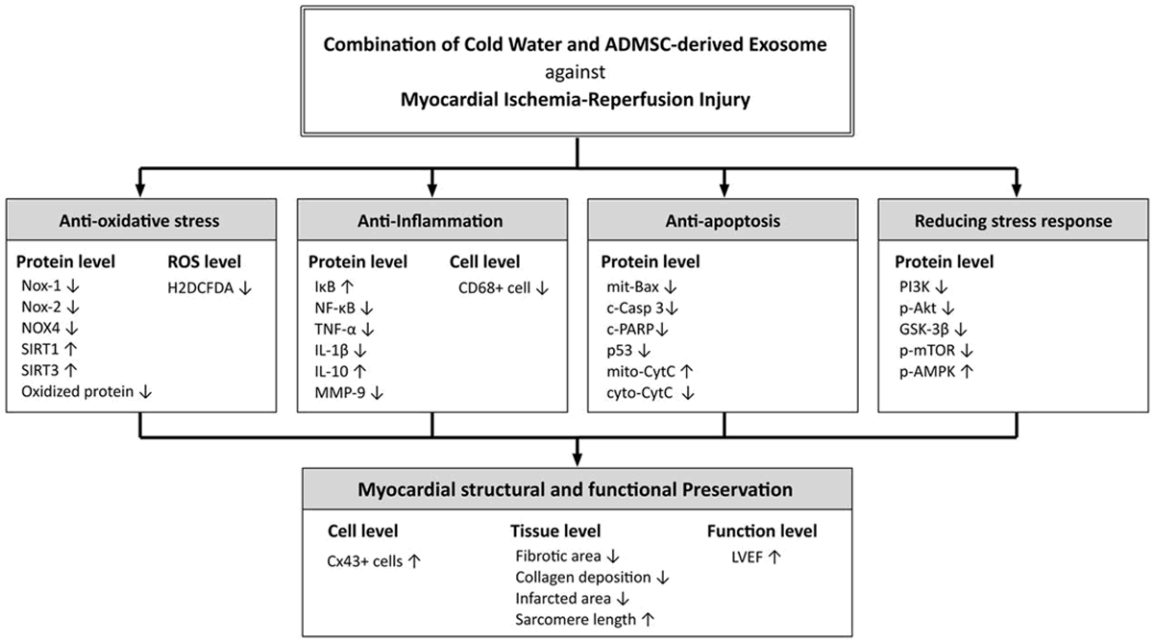

Figure 9. Proposed mechanisms underlying the positive therapeutic effects of CW-Exo preserved heart function in a setting of ischemia-reperfusion myocardial injury.

ing in the present study was that CW-Exo therapy downregulated the cell-stress response [i.e., (PI3K/Akt/GSK3β and p-m-TOR/p-AMKP)], sarcomere length, oxidative-stress and inflammatory signaling pathway as well as upregulated cell to cell gap junction, antioxidant (i.e., SIRT1, SIRT3) and anti-inflammatory (IL-10) biomarkers. In this way, our findings, in addition to corroborating with those from previous studies [30-32, 38-41], could once again explain why the functional (i.e., preserved LVEF and connexin 43) and cardiac architectural (attenuated the infarcted/fibrotic/collagen-deposition areas/sarcomere length) integrities were notably safeguarded in IR animals treated by CW-Exo regimen.

Study limitation

This study has limitations. First, despite the short-term results were attractive and promising, the study period lasted only five days. Certainly, the long-term outcome remains unclear. Second, although extensive works had been done in the present study, the exact underlying mechanisms of CW-Exo therapy on protecting the heart from acute IR injury are not fully identified. The proposed mechanisms underlying the observed protective effects of CW-Exo treatment against IR-induced cardiac damage based on our findings have been summarized in supplemental **Figure 9**.

In conclusion, CW-Exo therapy offered reliable benefit on protecting the heart against IR-induced myocardial damage mainly through regulating the cell-stress response, oxidative-stress and inflammatory signaling pathways.

Acknowledgements

This study was supported by a program grant from Chang Gung Memorial Hospital, Chang Gung University (Grant number: CMRPG8G11-51).

Disclosure of conflict of interest

None.

Address correspondence to: Drs. Hon-Kan Yip and Han-Tan Chai, Division of Cardiology, Department of Internal Medicine, Kaohsiung Chang Gung Memorial Hospital and Chang Gung University College of Medicine, Kaohsiung 83301, Taiwan. Tel: +886-7-7317123; Fax: +886-7-7322402; E-mail: han.gung@msa.hinet.net (HKY); chaiht@mail.cgmh.org.tw (HTC)

References

[1] GUSTO Angiographic Investigators. The effects of tissue plasminogen activator, streptokinase, or both on coronary-artery patency, ventricular

function, and survival after acute myocardial infarction. N Engl J Med 1993; 329: 1615-1622.
[2] Stone GW, Brodie BR, Griffin JJ, Morice MC, Costantini C, St Goar FG, Overlie PA, Popma JJ, McDonnell J, Jones D, O'Neill WW and Grines CL. Prospective, multicenter study of the safety and feasibility of primary stenting in acute myocardial infarction: in-hospital and 30-day results of the PAMI stent pilot trial. Primary angioplasty in myocardial infarction stent pilot trial investigators. J Am Coll Cardiol 1998; 31: 23-30.
[3] Yip HK, Chen MC, Chang HW, Hang CL, Hsieh YK, Fang CY and Wu CJ. Angiographic morphologic features of infarct-related arteries and timely reperfusion in acute myocardial infarction: predictors of slow-flow and no-reflow phenomenon. Chest 2002; 122: 1322-1332.
[4] Braunwald E and Kloner RA. Myocardial reperfusion: a double-edged sword? J Clin Invest 1985; 76: 1713-1719.
[5] Moens AL, Claeys MJ, Timmermans JP and Vrints CJ. Myocardial ischemia/reperfusion-injury, a clinical view on a complex pathophysiological process. Int J Cardiol 2005; 100: 179-190.
[6] Kim JS, Jin Y and Lemasters JJ. Reactive oxygen species, but not Ca2+ overloading, trigger pH- and mitochondrial permeability transition-dependent death of adult rat myocytes after ischemia-reperfusion. Am J Physiol Heart Circ Physiol 2006; 290: H2024-2034.
[7] Yellon DM and Hausenloy DJ. Myocardial reperfusion injury. N Engl J Med 2007; 357: 1121-1135.
[8] Eltzschig HK and Eckle T. Ischemia and reperfusion–from mechanism to translation. Nat Med 2011; 17: 1391-1401.
[9] Kloner RA, Ellis SG, Lange R and Braunwald E. Studies of experimental coronary artery reperfusion. Effects on infarct size, myocardial function, biochemistry, ultrastructure and microvascular damage. Circulation 1983; 68: 18-15.
[10] Ito H, Maruyama A, Iwakura K, Takiuchi S, Masuyama T, Hori M, Higashino Y, Fujii K and Minamino T. Clinical implications of the 'no reflow' phenomenon. A predictor of complications and left ventricular remodeling in reperfused anterior wall myocardial infarction. Circulation 1996; 93: 223-228.
[11] Chen YS, Chao A, Yu HY, Ko WJ, Wu IH, Chen RJ, Huang SC, Lin FY and Wang SS. Analysis and results of prolonged resuscitation in cardiac arrest patients rescued by extracorporeal membrane oxygenation. J Am Coll Cardiol 2003; 41: 197-203.
[12] Rokos IC, Larson DM, Henry TD, Koenig WJ, Eckstein M, French WJ, Granger CB and Roe MT. Rationale for establishing regional ST-elevation myocardial infarction receiving center (SRC) networks. Am Heart J 2006; 152: 661-667.
[13] Rokos IC, French WJ, Koenig WJ, Stratton SJ, Nighswonger B, Strunk B, Jewell J, Mahmud E, Dunford JV, Hokanson J, Smith SW, Baran KW, Swor R, Berman A, Wilson BH, Aluko AO, Gross BW, Rostykus PS, Salvucci A, Dev V, McNally B, Manoukian SV and King SB 3rd. Integration of pre-hospital electrocardiograms and ST-elevation myocardial infarction receiving center (SRC) networks: impact on door-to-balloon times across 10 independent regions. JACC Cardiovasc Interv 2009; 2: 339-346.
[14] De Scheerder I, Vandekerckhove J, Robbrecht J, Algoed L, De Buyzere M, De Langhe J, De Schrijver G and Clement D. Post-cardiac injury syndrome and an increased humoral immune response against the major contractile proteins (actin and myosin). Am J Cardiol 1985; 56: 631-633.
[15] Lange LG and Schreiner GF. Immune mechanisms of cardiac disease. N Engl J Med 1994; 330: 1129-1135.
[16] Frangogiannis NG, Smith CW and Entman ML. The inflammatory response in myocardial infarction. Cardiovasc Res 2002; 53: 31-47.
[17] Hoffman JW Jr, Gilbert TB, Poston RS and Silldorff EP. Myocardial reperfusion injury: etiology, mechanisms, and therapies. J Extra Corpor Technol 2004; 36: 391-411.
[18] Frangogiannis NG. The immune system and cardiac repair. Pharmacol Res 2008; 58: 88-111.
[19] Lambert JM, Lopez EF and Lindsey ML. Macrophage roles following myocardial infarction. Int J Cardiol 2008; 130: 147-158.
[20] Tsutsui H, Kinugawa S and Matsushima S. Mitochondrial oxidative stress and dysfunction in myocardial remodelling. Cardiovasc Res 2009; 81: 449-456.
[21] Kalogeris T, Baines CP, Krenz M and Korthuis RJ. Cell biology of ischemia/reperfusion injury. Int Rev Cell Mol Biol 2012; 298: 229-317.
[22] Chuah SC, Moore PK and Zhu YZ. S-allylcysteine mediates cardioprotection in an acute myocardial infarction rat model via a hydrogen sulfide-mediated pathway. Am J Physiol Heart Circ Physiol 2007; 293: H2693-2701.
[23] Misra MK, Sarwat M, Bhakuni P, Tuteja R and Tuteja N. Oxidative stress and ischemic myocardial syndromes. Med Sci Monit 2009; 15: RA209-219.
[24] Kalogeris T, Baines CP, Krenz M and Korthuis RJ. Ischemia/Reperfusion. Compr Physiol 2016; 7: 113-170.
[25] Kurisu K and Yenari MA. Therapeutic hypothermia for ischemic stroke; pathophysiology and future promise. Neuropharmacology 2018; 134: 302-309.
[26] Testori C, Sterz F, Behringer W, Haugk M, Uray T, Zeiner A, Janata A, Arrich J, Holzer M and Losert H. Mild therapeutic hypothermia is as-

sociated with favourable outcome in patients after cardiac arrest with non-shockable rhythms. Resuscitation 2011; 82: 1162-1167.
[27] Kim YM, Yim HW, Jeong SH, Klem ML and Callaway CW. Does therapeutic hypothermia benefit adult cardiac arrest patients presenting with non-shockable initial rhythms? A systematic review and meta-analysis of randomized and non-randomized studies. Resuscitation 2012; 83: 188-196.
[28] Perman SM, Grossestreuer AV, Wiebe DJ, Carr BG, Abella BS and Gaieski DF. The utility of therapeutic hypothermia for post-cardiac arrest syndrome patients with an initial non-shockable rhythm. Circulation 2015; 132: 2146-2151.
[29] Chan PS, Berg RA, Tang Y, Curtis LH, Spertus JA; American Heart Association's Get With the Guidelines-Resuscitation Investigators. Association between therapeutic hypothermia and survival after in-hospital cardiac arrest. JAMA 2016; 316: 1375-1382.
[30] Diestel A, Roessler J, Berger F and Schmitt KR. Hypothermia downregulates inflammation but enhances IL-6 secretion by stimulated endothelial cells. Cryobiology 2008; 57: 216-222.
[31] Sakurai T, Itoh K, Higashitsuji H, Nonoguchi K, Liu Y, Watanabe H, Nakano T, Fukumoto M, Chiba T and Fujita J. Cirp protects against tumor necrosis factor-alpha-induced apoptosis via activation of extracellular signal-regulated kinase. Biochim Biophys Acta 2006; 1763: 290-295.
[32] Qin J, Mai Y, Li Y, Jiang Z and Gao Y. Effect of mild hypothermia preconditioning against low temperature (4 degrees C) induced rat liver cell injury in vitro. PLoS One 2017; 12: e0176652.
[33] Zhou Y, Xu H, Xu W, Wang B, Wu H, Tao Y, Zhang B, Wang M, Mao F, Yan Y, Gao S, Gu H, Zhu W and Qian H. Exosomes released by human umbilical cord mesenchymal stem cells protect against cisplatin-induced renal oxidative stress and apoptosis in vivo and in vitro. Stem Cell Res Ther 2013; 4: 34.
[34] Chen HH, Lai PF, Lan YF, Cheng CF, Zhong WB, Lin YF, Chen TW and Lin H. Exosomal ATF3 RNA attenuates pro-inflammatory gene MCP-1 transcription in renal ischemia-reperfusion. J Cell Physiol 2014; 229: 1202-1211.
[35] Fleig SV and Humphreys BD. Rationale of mesenchymal stem cell therapy in kidney injury. Nephron Clin Pract 2014; 127: 75-80.
[36] Zou X, Zhang G, Cheng Z, Yin D, Du T, Ju G, Miao S, Liu G, Lu M and Zhu Y. Microvesicles derived from human Wharton's Jelly mesenchymal stromal cells ameliorate renal ischemia-reperfusion injury in rats by suppressing CX3CL1. Stem Cell Res Ther 2014; 5: 40.
[37] Ko SF, Yip HK, Zhen YY, Lee CC, Lee CC, Huang CC, Ng SH and Lin JW. Adipose-derived mesenchymal stem cell exosomes suppress hepatocellular carcinoma growth in a rat model: apparent diffusion coefficient, natural killer T-cell responses, and histopathological features. Stem Cells Int 2015; 2015: 853506.
[38] Chang CL, Sung PH, Chen KH, Shao PL, Yang CC, Cheng BC, Lin KC, Chen CH, Chai HT, Chang HW, Yip HK and Chen HH. Adipose-derived mesenchymal stem cell-derived exosomes alleviate overwhelming systemic inflammatory reaction and organ damage and improve outcome in rat sepsis syndrome. Am J Transl Res 2018; 10: 1053-1070.
[39] Chen KH, Chen CH, Wallace CG, Yuen CM, Kao GS, Chen YL, Shao PL, Chen YL, Chai HT, Lin KC, Liu CF, Chang HW, Lee MS and Yip HK. Intravenous administration of xenogenic adipose-derived mesenchymal stem cells (ADMSC) and ADMSC-derived exosomes markedly reduced brain infarct volume and preserved neurological function in rat after acute ischemic stroke. Oncotarget 2016; 7: 74537-74556.
[40] Lin KC, Yip HK, Shao PL, Wu SC, Chen KH, Chen YT, Yang CC, Sun CK, Kao GS, Chen SY, Chai HT, Chang CL, Chen CH and Lee MS. Combination of adipose-derived mesenchymal stem cells (ADMSC) and ADMSC-derived exosomes for protecting kidney from acute ischemia-reperfusion injury. Int J Cardiol 2016; 216: 173-185.
[41] Sun CK, Chen CH, Chang CL, Chiang HJ, Sung PH, Chen KH, Chen YL, Chen SY, Kao GS, Chang HW, Lee MS and Yip HK. Melatonin treatment enhances therapeutic effects of exosomes against acute liver ischemia-reperfusion injury. Am J Transl Res 2017; 9: 1543-1560.
[42] Chua S, Lee FY, Tsai TH, Sheu JJ, Leu S, Sun CK, Chen YL, Chang HW, Chai HT, Liu CF, Lu HI and Yip HK. Inhibition of dipeptidyl peptidase-IV enzyme activity protects against myocardial ischemia-reperfusion injury in rats. J Transl Med 2014; 12: 357.
[43] Leu S, Sun CK, Sheu JJ, Chang LT, Yuen CM, Yen CH, Chiang CH, Ko SF, Pei SN, Chua S, Youssef AA, Wu CJ and Yip HK. Autologous bone marrow cell implantation attenuates left ventricular remodeling and improves heart function in porcine myocardial infarction: an echocardiographic, six-month angiographic, and molecular-cellular study. Int J Cardiol 2011; 150: 156-168.